

## Decision Tree Based Expert System for Power Factor Improvement Under Distorted and Unbalanced Current Conditions

**Abstract.** This paper proposes a methodology to identify the reactive and harmonic compensation in three-phase power systems. Considering the behavior of power factor, current and voltage harmonic distortion, unbalance factors and reactive power daily variation, the developed tool is able to select two suitable solutions for power factor correction on the installation under analysis. The results gathered from computational simulations, as well as from measuring an industrial facility are presented and discussed. Based on specialist knowledge the developed tool may be very useful for finding the correct compensation solution quickly even manipulating a large amount of data.

**Streszczenie.** Artykuł proponuje metodykę identyfikacji kompensacji mocy biernej i harmonicznyc. Biorąc pod uwagę dzienne zmiany współczynnika mocy, odkształcenia prądów i napięć, współczynników niezrównoważenia oraz mocy biernej, przedstawiona metoda jest w stanie wybrać dwa odpowiednie rozwiązania dla poprawy współczynnika mocy w analizowanym systemie. W artykule przedstawione są i przedyskutowane wyniki zebrane z modelowania komputerowego oraz z pomiarów na obiektach przemysłowych. W oparciu o specjalistyczną wiedzę, przedstawiona metoda może być bardzo użyteczna w szybkim poszukiwaniu poprawnej kompensacji, nawet w przypadku dużej ilości danych. **System ekspercki poprawy współczynnika mocy oparty na Drzewie Decyzyjnym w warunkach odkształceń i asymetrii prądów**

**Keywords:** Active Compensators, Passive Compensators, Power Factor, Reactive and Harmonics Compensation, Selective compensation, STD-1459-2010.

**Słowa kluczowe:** Kompensatory aktywne, kompensatory pasywne, współczynnik mocy, kompensacja harmonicznyc i mocy biernej, kompensacja selektywna, STD-1459-2010

### Introduction

One of the most relevant discussions regarding power quality, mostly because it does not only concern technical, but also economic aspects is the power factor (PF) definition [1].

The PF is commonly used to quantify and charge the reactive power present in electric systems, even though numerous studies have shown that its definition requires deep consideration when applied to nonsinusoidal and unbalanced systems [2-5]. In other words, deviations from the ideal conditions in an electric system generate results that may lead to errors in power factor evaluation and consequently, on the revenue metering [6-10]. Thus, considering the great increase in nonlinear loads, primary causes of distortions and other disturbances in the electric system, it is imperative to adjust the measuring and revenue metering methodologies for power factor consideration.

Therefore, starting from conventional power factor definitions, which are usually based on purely sinusoidal and balanced systems, this paper aims to define an automatic power factor compensation methodology for three-phase electric power systems under distorted and or unbalanced current conditions. Thus, the proposed methodology considers the power factor, and the voltage and current quantities related to nonsinusoidal and unbalanced systems [8],[11]. Furthermore, the proposed automatic apparatus is able to perform the measuring, the analysis of available data and also to suggest two proper solutions for PF compensation in three-phase sinusoidal and/or nonsinusoidal conditions in the presence of balanced or unbalanced loads.

In order to validate the proposed methodology, some computational simulations were carried out using the IEEE 13-node test feeder. Besides, a one-week measurement was performed in a metallurgical facility composed by linear and nonlinear loads, with 11.9 kV, 2 MVA, 60 Hz. The results obtained are presented and discussed in the following.

### Proposed methodology

Fig. 1 describes the proposed methodology. Voltage and current signals are measured through a virtual instrument that will process the signals through a data acquisition board, and store the data of seven consecutive days. Then, the stored data are classified and processed through a decision tree algorithm, which selects the two most suitable solutions for reactive and harmonic compensation.

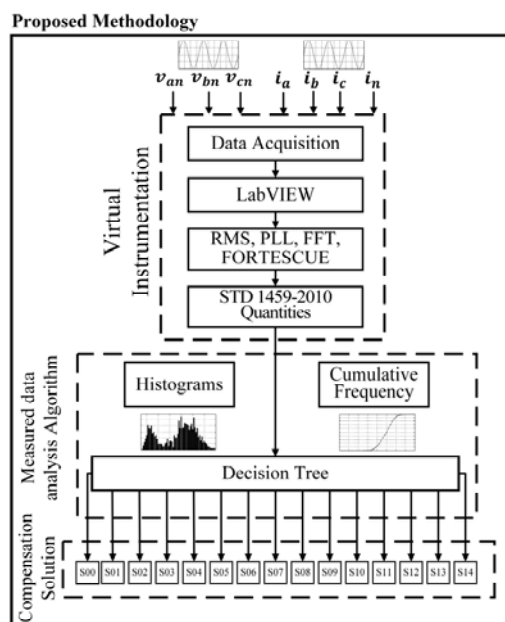


Fig.1. Proposed methodology.

#### A. The Virtual Instrument

Using an object-oriented programming language (LabView® from National Instruments), an interface of data acquisition, was developed for real time processing of electric quantities extracted from voltage and current signals from the grid [12].

Digital processing algorithms were implemented to calculate rms and average quantities using moving average filter, so all quantities are calculated with a 12 kHz sampling frequency, but the data are stored once per minute.

Power factor and power quantities are calculated according to STD 1459-2010 definition [9]. Since this standard proposes the separation of fundamental components of voltage, current and power, a fundamental component detector based on PLL (Phase Locked Loop) algorithm was implemented [12,13].

Fig. 2 presents the measurement system and the virtual instrument. It is worth highlighting that the virtual instrument developed is capable of processing and store a large amount of data measured every minute.

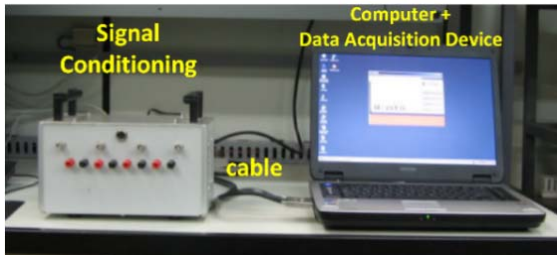


Fig.2. Virtual instrument developed.

### B. Data Analysis Algorithm

Since all extracted information is stored, an automatic analysis methodology is used to classify the parameters and indicators according to their limits. This approach is based on previous specialist knowledge and allows the possibility of determining distinct solutions of reactive and harmonic compensation.

Fig. 3 shows the selective diagram used to classify the compensation cases as a function of the parameters ( $PF_e, KI_1^-, KI_1^0, THD_I, THD_V$  and  $\Delta Q_1^+$ ) that violated their respective limits. The basic idea is to sequentially test these quantities against their respective pre-established limits using a decision tree as decision-maker process [14], differently from other methodology proposed in [15] that applies a fuzzy decision-maker.

In order to consider the temporal variations of the parameters, the analysis program obtains the daily histogram taking into account the stored data. So, at the end of the day the  $PF_e, KI_1^-, KI_1^0, THD_I, THD_V$  and  $Q_1^+$  histograms are available. Then, it is possible to have the percentage of time during the pre-established limits are violated along the day. This information becomes useful to evaluate the relative importance of the long-term violations.

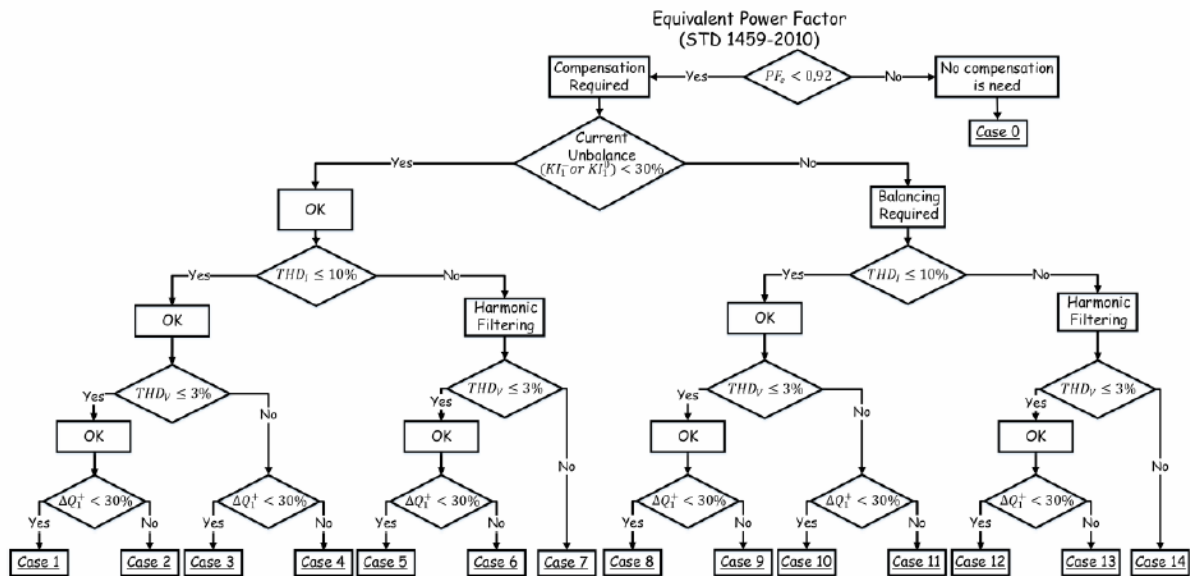


Fig.3. Decision tree of the proposed methodology.

Table 1. Possible Compensation Solutions.

Case	Description
00	No compensation is need;
01	Three-Phase Capacitive Bank;
02	Variable Three-Phase Capacitive Bank;
03	Three-Phase Capacitive Bank + series reactor;
04	Variable Three-Phase Capacitive Bank + series reactor;
05	Fixed Three-Phase Passive Filter + Fixed Three-Phase Capacitive Bank;
06	Variable Three-Phase Passive Filter + Variable Three-Phase Capacitive Bank;
07	Three-Phase – Three wire – Shunt Active Power Filter;
08	Fixed Independent (per-phase) reactive compensation (capacitors/inductors);
09	Variable Independent Reactive Compensation (capacitors/inductors);
10	Fixed Independent (per-phase) reactive compensation (capacitors/inductors) + insertion of series reactor or slight changing in filter frequency;
11	Variable Independent (per-phase) reactive compensation (capacitors/inductors) + insertion of series reactor or slight

	changing in filter frequency;
12	Fixed Independent per-phase Passive Filter + Independent Reactive Bank;
13	Variable Independent per-phase Passive Filter + Independent Reactive Bank;
14	Three-Phase – Four wire – Shunt Active Power Filter.

### C. Compensation Solutions

There are several possibilities and types of compensators used for power factor correction, load balancing or reducing the voltage and current distortions. However, in specific situations a given compensator that would be perfectly applicable may be damaging or less effective. An example would be the tuned passive filters with distorted voltages or in the case of parallel active filter, with sinusoidal wave synthesis, in a deteriorated PCC (Point Common Coupling).

For this reason, the diagram in Fig. 3 seeks to provide a compensation solution through a decision tree. Starting from the test of each parameter measured at every minute

and with pre-established limits, the results are classified according to the possible solutions presented in Table 1.

Subsequently, the algorithm finds the two most incident solutions in the given period and designates the two main solutions for compensation.

### Simulation results

The methodology presented in Fig.1 was assessed and discussed by means of the IEEE 13 node test feeder, which was simulated on PSCAD. Several simulations of different compensation cases were performed, in order to verify the classifier performance (Fig.3) and the effectiveness of the proposed solutions. In the node 634, a nonlinear load (6 pulse controlled rectifier operating with  $45^\circ$ ) was inserted in order to generate current harmonics, as shown in Fig. 4.

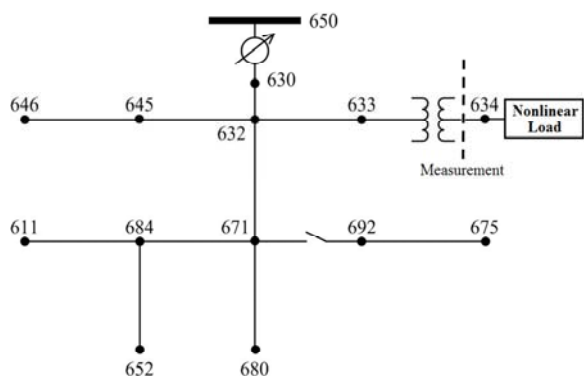


Fig.4. Single-line diagram of the IEEE 13 bus test system.

#### A. Preliminary assessment

The instantaneous voltages and currents were measured at node 634. Fig. 5(a) shows the instantaneous voltage  $v_{an}$  and current  $i_a$ , while Fig. 5(b) shows their harmonic contents. Note the presence of low order harmonics - 5<sup>th</sup>, 7<sup>th</sup>, 11<sup>th</sup>, 13<sup>th</sup> and 17<sup>th</sup>. The THD of voltage  $v_a$  and current  $i_a$  were 0.93% and 12.54%, respectively.

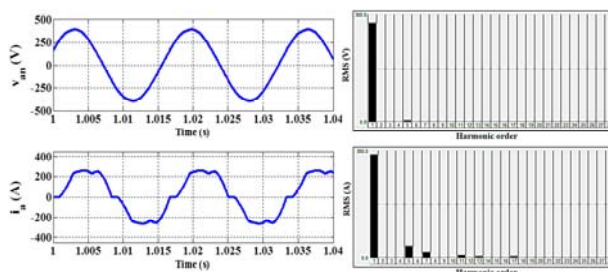


Fig.5 Voltage and current at 634 bus before compensation. (a) Time domain waveforms. (b) Frequency spectra.

The evolution of the equivalent power factor measured in node 634 is shown in Fig. 6(a). Through the curve of accumulated frequency it is possible to determine that the power factor is below 0.92 (adopted limit), Fig. 6(b). This is a "minimum limits" violation curve, which means that during 100% of the measuring period the power factor has violated the standard limits, thus some correction in the power factor is needed. Fig. 6(c) shows the evolution of current distortion. As can be seen, there is a high level of current distortion due to nonlinear load. Fig. 6(d) shows the probability histogram for harmonic current distortion levels. It represents a "maximum limits" violation curve, which means that the equivalent current total harmonic distortion is above 10% during 100% of the measuring period.

Table 2 shows some PQ indices and power terms according to the IEEE 1459-2010 [9]. It is important to underline that the values were obtained from the

instantaneous current and voltage waveforms measured at 634 bus.

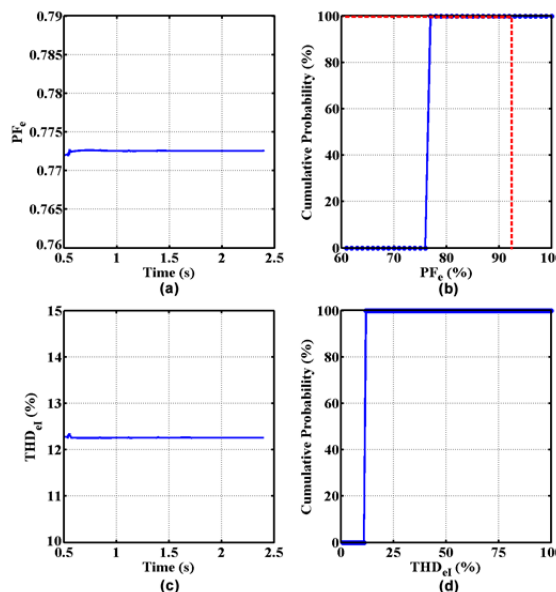


Fig.6. Parameters evolution and Histograms before compensation at 634 bus. (a) Equivalent power factor. (b) Equivalent power factor histogram. (c) Equivalent current total harmonic distortion. (d) Equivalent current total harmonic distortion histogram.

Note from Table 2 that power factor at node 634 violates the acceptable limits ( $PF_e = 0.77$ ). This is due to the non-linear load behavior. Moreover, the current equivalent total harmonic distortion has significant level of 12.25%. The harmonic active power ( $P_H = -49.34W < 0$ ) is supplied by the load and injected into the power system. Therefore, a compensation solution is needed at node 634.

Table 2. Voltage, current and power magnitudes before compensation.

$V_{an} = 277.45 \text{ V}$	$V_{bn} = 282.50 \text{ V}$	$V_{cn} = 279.84 \text{ V}$
$V_e = 279.94 \text{ V}$	$V_{e1} = 279.93 \text{ V}$	$V_{eH} = 2.81 \text{ V}$
$V_1^+ = 279.91 \text{ V}$	$V_1^- = 3.58 \text{ V}$	$V_1^0 = 0.93 \text{ V}$
	$V_1^-/V_1^+ = 1.28 \%$	$V_1^0/V_1^+ = 0.33 \%$
$I_{an} = 192.74 \text{ A}$	$I_{bn} = 196.09 \text{ A}$	$I_{cn} = 196.66 \text{ A}$
$I_e = 195.17 \text{ A}$	$I_{e1} = 193.73 \text{ A}$	$I_{eH} = 23.74 \text{ A}$
$I_1^+ = 193.72 \text{ A}$	$I_1^- = 2.51 \text{ A}$	$I_1^0 = 0.00 \text{ A}$
	$I_1^-/I_1^+ = 1.30 \%$	$I_1^0/I_1^+ = 0.00 \%$
$S_e = 126635.90 \text{ VA}$	$S_{e1} = 162699.30 \text{ VA}$	$S_{eN} = 19856.44 \text{ VA}$
$S_1^+ = 162671.90 \text{ VA}$	$P_1^+ = 126658.70 \text{ W}$	$Q_1^+ = 102077.10 \text{ var}$
$P_1 = 126658.70 \text{ W}$	$P = 126635.90 \text{ W}$	$S_{H1} = 2982.73 \text{ VA}$
$PF_e = 0.7726$	$PF_1 = 0.7786$	$PF_1^+ = 0.7786$
	$THD_{eV} = 1.00 \%$	$THD_{eI} = 12.25 \%$
$D_{eV} = 1632.91 \text{ VA}$	$D_{eI} = 19936.77 \text{ VA}$	$S_{eH} = 200.09 \text{ VA}$
	$D_{eH} = 193.91$	$P_H = -49.34 \text{ W}$

#### B. Mitigation Analysis

The following compensation solution is obtained through the proposed methodology:

- **First solution:** Fixed Three-Phase Passive Filter + Fixed Three-Phase Capacitive Bank;
- **Second solution:** Three-Phase – Three wire – Shunt Active Power Filter.

Table 3 shows the percentage of violation limits calculated by means of the probability histograms. Note that  $PF_e$  has been violated during 100% of the measurement period, while  $THD_I$  exceeded their limit during 100% of the period. In this case, the classification algorithm suggested the correct solution (case 05).

Table 3. Percentage of violation limits based on measurement period.

$PF_e$ (%)	100.00
$KI_1^-$ (%)	0.00
$KI_1^0$ (%)	0.00
$THD_V$ (%)	100.00
$THD_V$ (%)	0.00
$Q_{iAVG}^-30\%$	0.00
$Q_{iAVG}^+30\%$	0.00

From the foregoing proposed solution, a new simulation was made in order to verify the effectiveness of first compensation solution proposed by the algorithm.

Fig. 7(a) presents the instantaneous voltage  $v_{an}$  and current  $i_a$  measured at node 634 after the three-phase passive filter installation. Notice from Fig. 7(b) that the impact of current harmonic distortion was minimized.

As can be seen in Fig. 7(b) there has been a mitigation of 3<sup>rd</sup> harmonic order and a decrease of 5<sup>th</sup> and 7<sup>th</sup> harmonic order. Consequently, the power factor results above 0.92 as shown in Table 4. Moreover, the equivalent current total harmonic distortion decreased from 12.25% to 5.33%.

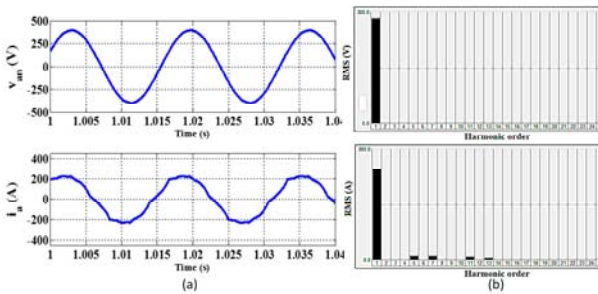


Fig.7 Voltage and current at 634 bus after compensation. (a) Time domain waveforms. (b) Frequency spectra.

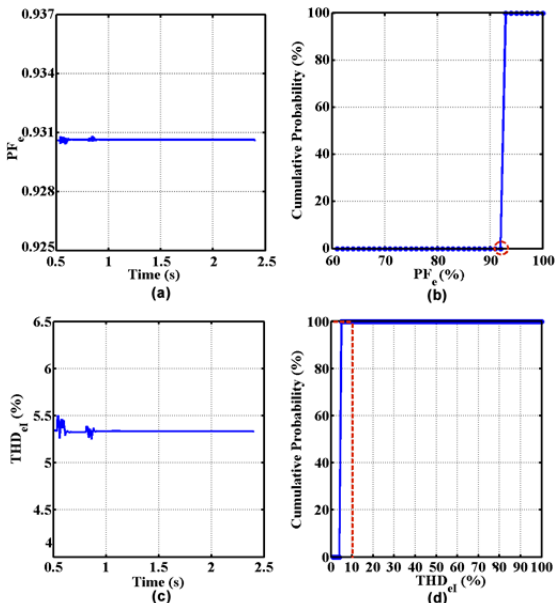


Fig.8 Parameters evolution and Histograms after compensation at 634 bus. (a) Equivalent power factor. (b) Equivalent power factor histogram. (c) Equivalent current total harmonic distortion. (d) Equivalent current total harmonic distortion histogram.

The new evolution of the equivalent power factor measured in node 634 is shown in Fig. 8(a). By analysing the curve of accumulated frequency, it is possible to verify that the proposed solution improved the power factor during 100% of the measuring period. In addition, the current harmonic distortion level is below 10% during 100% of the measuring period, Fig. 8(d).

Table 4 shows some PQ indices and power terms after compensation. Note that the power factor was improved due to the three phase passive filter installation, as well as current harmonic distortion.

In the following section, it is presented an application of the proposed methodology on an industrial facility with power quality issues.

Table 4. Load voltage, current and power magnitudes after compensation.

$V_{an} = 280.50$ V	$V_{bn} = 283.98$ V	$V_{cn} = 281.34$ V
$V_e = 281.94$ V	$V_{e1} = 281.95$ V	$V_{eH} = 1.28$ V
$V_1^+ = 281.93$ V	$V_1^- = 3.14$ V	$V_1^0 = 1.52$ V
	$V_1^-/V_1^+ = 1.11$ %	$V_1^0/V_1^+ = 0.54$ %
$I_{an} = 163.26$ A	$I_{bn} = 166.20$ A	$I_{cn} = 166.92$ A
$I_e = 165.47$ A	$I_{e1} = 165.24$ A	$I_{eH} = 8.80$ A
$I_1^+ = 165.20$ A	$I_1^- = 2.78$ A	$I_1^0 = 0.98$ A
	$I_1^-/I_1^+ = 1.68$ %	$I_1^0/I_1^+ = 0.59$ %
$S_e = 139958.80$ VA	$S_{e1} = 139765.10$ VA	$S_{eN} = 7361.90$ VA
$S_1^+ = 139725.60$ VA	$P_1^+ = 130234.80$ W	$Q_1^+ = 50617.54$ var
$P_1 = 130255.70$ W	$P = 130243.60$ W	$S_{U1} = 3323.24$ VA
$PF_e = 0.9306$	$PF_1 = 0.9320$	$PF_1^+ = 0.9321$
	$THD_{eV} = 0.45$ %	$THD_{eI} = 5.33$ %
$D_{eV} = 633.80$ VA	$D_{eI} = 7445.63$ VA	$S_{eH} = 33.76$ VA
	$D_{eH} = 1.64$	$P_H = -12.16$ W

### Case study using experimental data

In order to validate the proposed methodology, it was considered a data set of 10 days of measurements in a metallurgical facility, composed by linear and nonlinear loads, with a supply voltage of 11.9 kV, 2 MVA, 60 Hz. This installation presents a large quantity of nonlinear loads, adjustable speed drives (ASD) and induction electrical machines, which result in an extensive amount of load with current harmonics source behavior.

#### A. Data from the second day of measurements

Fig 9. presents the evolution of the equivalent power factor measured on the second day of analysis, which corresponds to a working day at the industrial facility (Wednesday). It can be verified that the power factor is below 0.92 from midnight to 4pm, which accounts for 70% of the period measured on this day.

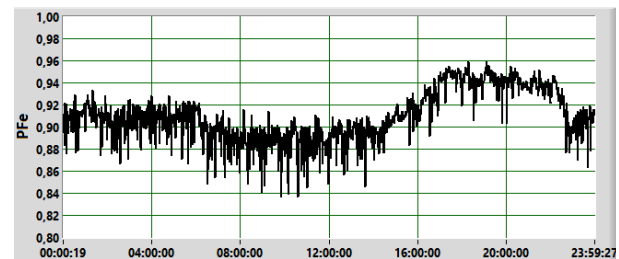


Fig.9 Equivalent power factor ( $PF_e$ ) behavior for second day of measurements.

Fig. 10 represents the curve of cumulative frequency of ( $PF_e$ ). This is a “minimum limits” violation curve, i. e., the power factor is below 0.92 during 69.87% of the day.

In order to verify the load unbalance condition in the facility, Fig. 11 shows the negative sequence unbalance factor ( $KI_1^-$ ) for the load currents. It indicates that the loads are relatively well distributed throughout the phases, because the values are below the 30% of the limit adopted for the current unbalance.

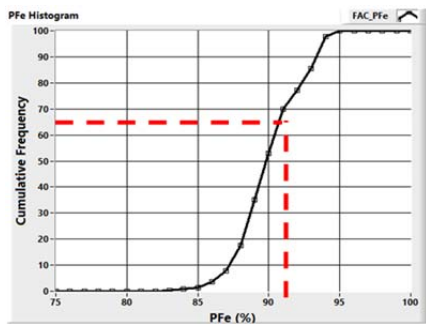


Fig. 10 Equivalent power factor histogram for second day of measurements.

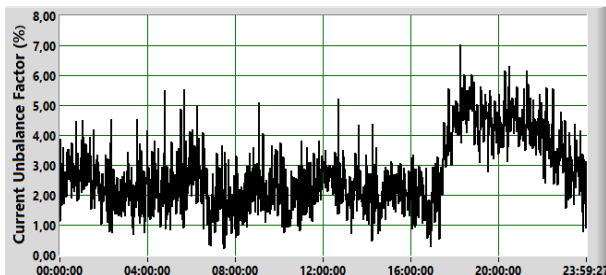


Fig. 11 Equivalent power factor histogram for second day of measurements.

It is important to notice that the virtual instrument processes the temporal decomposition of the voltage and current signals, separating and calculating the fundamental components and also the positive sequence for voltage, current and power. Fig. 12 shows the positive-sequence fundamental reactive power ( $Q_1^+$ ), measured during 24 hours. Variations during the measuring interval can be noticed. The analysis algorithm checks if the reactive variations are above or below 30% of the mean value. For this day, the average ( $Q_1^+$ ) was 287.03 kvar. The inferior limit for the violation of the reactive variation was only 20.71% of the measuring period whereas the superior limit was 10.88%.

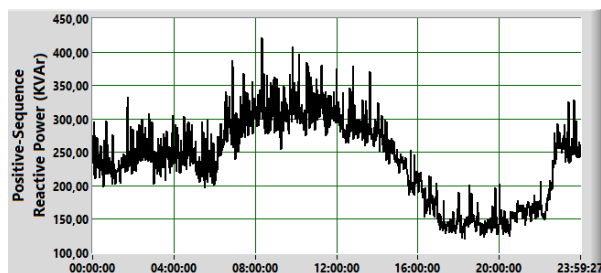


Fig. 12. Positive-sequence reactive power ( $Q_1^+$ ) behavior for second day of measurements.

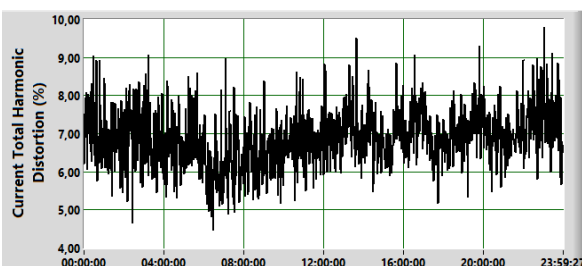


Fig. 13. Current total harmonic distortion behavior ( $THD_{1a}$ ) for second day of measurements.

Fig. 13 shows the evolution of current total harmonic distortion in one phase. Note that harmonic distortion was

below 10% (pre-established limit) during the whole period.

For the second day of measuring, the tool suggested **solution 01** (Three-phase fixed capacitors bank) as the highest incidence solution. The second option would be **solution 00**.

#### B. Data from the sixth day of measurements

The sixth day was a Sunday. It was chosen because the load profile was significantly different from the other days, based on the absence of linear loads, resulting, basically, in nonlinear loads.

Fig. 14 features the evolution of the equivalent power factor for the sixth day, during which its value surpasses the minimum limit 68% of the time.

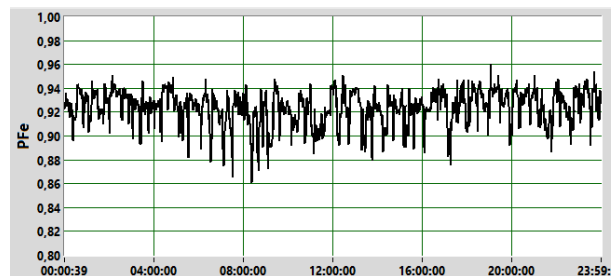


Fig. 14. Equivalent power factor ( $PFe$ ) behavior for sixth day of measurements.

Fig. 15 indicates the importance of evaluating the weekends, because an elevated current distortion can be noticed, which violates the limit ( $THD_1 = 10\%$ ) for the entire time.

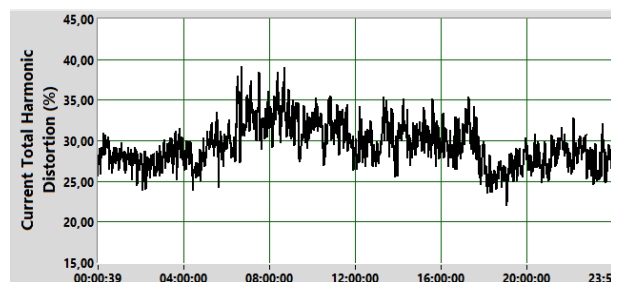


Fig. 15. Current total harmonic distortion behavior ( $THD_{1a}$ ) for sixth day of measurements.

With the facility nearly in standby, the demand for reactive power falls below 10% of the daily value for workdays, as in Fig. 16.

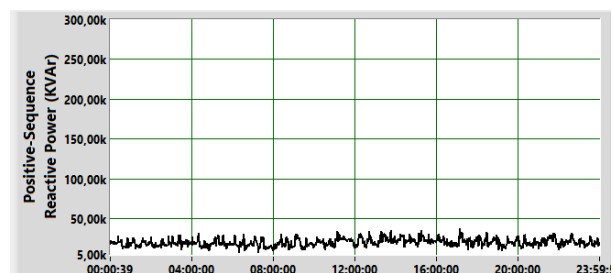


Fig. 16. Positive-sequence reactive power ( $Q_1^+$ ) behavior for sixth day of measurements.

For the sixth day of measuring, the tool provided **solution 00** (No compensation is need) as the highest occurring solution. The second would be **solution 05**. However, the compensation strategies are determined considering the suggested solutions during a period of several days or even weeks, as discussed in the following.

### C. Assessment of the monitoring period

From the suggestions gathered for each measuring day, an analysis of the load behavior during one week results in a good mid-term view.

From the 10-day data, it is safe to conclude that the two best options for compensation of the power factor appear in the following order:

1. a permanent bank of three-phase capacitors in order to maintain the power factor above 0.92. A 150kVAr bank matches the criteria for minimum reactive compensation, avoiding over compensation in days with normal production. However, the capacitors bank would have to be shut off during the weekends, when the facility has practically no loads.
2. the second recommendation suggests not doing the compensation, thus, accounting for the risks of keeping the power factor below 0.92 and being penalized by the utility. A comparison of installation costs and bank maintenance may indicate the time needed to pay off the investment

It is also worth noting that all the measuring was made at PCC. Because of that, the compensation solutions are suitable for the voltage level at that point.

### Conclusion

This paper proposed a possible methodology for defining power factor compensators in a considered PCC. The main focus is to provide an automatic tool for helping utility engineers and industrial consumers in their decision process, when choosing solutions for compensating the power factor.

The proposed tool is composed by a virtual instrument and a decision making process. The virtual instrument is able to perform the analysis of several signals simultaneously with high sampling and processing capabilities differently from conventional instruments, such as signal analyzers and power meters.

The decision process is based on several rules, which reproduce the human expertise in this area, in such a way the apparatus is very simple to operate and it can suggest suitable compensation solutions for a particular PCC.

Finally, it is important to highlight that the proposed methodology has no parallel in literature, a part from a correlated paper from the same group of authors, using a fuzzy decision maker instead of the decision tree proposed in this paper.

### Acknowledgement

The authors wish to express their gratitude to CPFL Energy, CNPq and the Brazilian agency CAPES for supporting this research.

### REFERENCES

- [1] Thomas K., Lai J.S., "Costs and benefits of harmonic current reduction for switch-mode power supplies in a commercial office building", *IEEE Transactions on Industry Applications*, vol.32, no.5, pp.1017,1025, Sep/Oct 1996.
- [2] Tenti P., Mattavelli P., Paredes H.K.M., "Conservative Power Theory, sequence components and accountability in smart grids", *Przeegląd Elektrotechniczny (Electrical Review)*, vol. 6, pp. 30-37, 2010.
- [3] Staudt V., "Fryze-Buchholz-Depenbrock: A Time-Domain Power Theory," *Przeegląd Elektrotechniczny (Electrical Review)*, no. 6, pp. 1-11, 2008.
- [4] Czarnecki L.S., "Currents' Physical Components (CPC) Concept: a Fundamental of Power Theory," *Przeegląd Elektrotechniczny (Electrical Review)* no. 6, pp. 28-37, 2008.
- [5] Willems J.L., "Reflections on Power Theories for Poly-Phase Nonsinusoidal Voltages and Currents," *Przeegląd Elektrotechniczny (Electrical Review)* no. 6, pp. 11-21, 2010.
- [6] Ferrero A., Peretto L. and Sasdelli R., "Revenue Metering in the Presence of Distortion and Unbalance: Myths and Reality," *IEEE Proceedings of the International Conference on Harmonics and Quality of Power*, pp. 42-47, 1998.
- [7] Tenti P., Paredes H.K.M., Marafão F.P., Mattavelli P., "Accountability and revenue metering in smart micro-grids," *IEEE International Workshop on Applied Measurements for Power Systems (AMPS)*, 2010, pp.74-79, Sept. 2010.
- [8] Marafão F.P., Deckmann S.M. and Marafão J.A.G., "Power Factor Analysis under Non-Sinusoidal and Unbalanced Systems," in *Proc. 2002 IEEE Proceedings of the International Conference on Harmonics and Quality of Power*, pp. 42-47.
- [9] *IEEE Standard Definitions for the Measurement of Electric Power Quantities Under Sinusoidal, Nonsinusoidal, Balanced, or Unbalanced Conditions*, IEEE Std 1459-2010, pp.1-50, March 19 2010.
- [10] Manjure D.P., Makram E.B., "Effect of nonlinearity and unbalance on power factor", *IEEE Power Engineering Society Summer Meeting*, vol.2, pp.956-962, vol. 2, 2000.
- [11] Marafão F. P., "Electrical Energy Analysis and Control Using Digital Signal Processing Techniques", PhD thesis, Dept. of Systems and Energy Control, University of Campinas, Brazil, 2004. (in Portuguese).
- [12] Moreira A.C., Deckmann S.M., Marafão F.P., Lima E.G. and Bini M.A., "Virtual Instrumentation Applied to the Implementation of IEEE STD 1459-2000 Power Definitions", *IEEE 36th Power Electronics Specialists Conference - PESC*, 2005.
- [13] Pádua M. S., Deckmann S. M., and Marafão F. P., "Frequency-Adjustable Positive Sequence Detector for Power Conditioning Applications", *IEEE 36th Power Electronics Specialists Conference - PESC*, 2005.
- [14] Equipment for automatic definition of reactive and/or current disturbances compensation using real-time measurements, by Deckmann S.M., Marafão F.P. and Moreira A.C. (2008, September 19). Patent PI0803478-8 (in Portuguese). [Online]. Available: [www.inpi.gov.br/portal/](http://www.inpi.gov.br/portal/)
- [15] Liberado E.V., Marafão F.P., Simões M.G., Souza W.A. de and Pomilio J.A., "Novel Expert System for Defining Power Quality Compensators," *Expert Systems With Applications*, vol. 42, March 2015, pp. 3562-3570.

**Authors:** Msc Alexandre C. Moreira, School of Electrical and Computer Engineering, Department of Electrical Energy Systems, University of Campinas, Unicamp/FEEC/DSEE, Av. Albert Einstein,400, 13083-852 Campinas, SP – Brazil; [alexandre.candido.moreira@gmail.com](mailto:alexandre.candido.moreira@gmail.com). Dr Sigmar M. Deckmann, School of Electrical and Computer Engineering, Department of Electrical Energy Systems, University of Campinas, Unicamp/FEEC/DSEE, Av. Albert Einstein,400, 13083-852 Campinas, SP – Brazil; [sigmar@fee.unicamp.br](mailto:sigmar@fee.unicamp.br). Dr. Fernando P. Marafão, Group of Automation and Integrated Systems, Unesp – Univ Estadual Paulista, Av. Três de Março,511, 18087-180 Sorocaba, SP - Brazil; [fmarafao@sorocaba.unesp.br](mailto:fmarafao@sorocaba.unesp.br). Dr. Luis C. P. da Silva, School of Electrical and Computer Engineering, Department of Electrical Energy Systems, University of Campinas, Unicamp/FEEC/DSEE, Av. Albert Einstein,400, 13083-852 Campinas, SP – Brazil; [lui@dsee.fee.unicamp.br](mailto:lui@dsee.fee.unicamp.br). Dr.Helmo K. M. Paredes, Group of Automation and Integrated Systems, Unesp – Univ Estadual Paulista, Av. Três de Março,511, 18087-180 Sorocaba, SP - Brazil; [hmorales@sorocaba.unesp.br](mailto:hmorales@sorocaba.unesp.br).